Proceedings of the Seventh International Conference on
Railway Technology: Research, Development and Maintenance
Edited by: J. Pombo
Civil-Comp Conferences, Volume 15, Paper 9.11
Civil-Comp Press, Edinburgh, United Kingdom, 2026
ISSN: 2753-3239, doi: 10.4203/ccc.15.9.11

Thermal Behaviour of Railway Brake Blocks: On-Track Temperature Measurements for Numerical Model Validation

N. Bosso[1], G. Borgi[2], M. Magelli[1], R. Pagano[1], L. Sabbatini[2] and N. Zampieri[1]

[1]Department of Mechanical and Aerospace Engineering, Politecnico di Torino, Italy
[2]SRT Smart Railway Technology, Fano (PU), Italy

Abstract

The widespread adoption of composite brake blocks on freight trains, driven by European regulations on rolling noise emissions, has led to new issues related to tread braking operations. The significantly lower thermal conductivity of composite materials with respect to traditional cast iron shoes can cause larger temperature increase on the wheel, raising concerns on thermal damage, wear mechanisms and wheel integrity. Therefore, the ability to predict the evolution of the thermal field with computationally efficient models represents a key challenge. This paper shows the validation of a simplified 2D finite element (FE) thermal model of a brake block with experimental data collected under real operating conditions. The model is developed in ANSYS considering a 2D plane geometry, to ensure computational efficiency. The model inputs, including the interface heat flux, are derived from onboard measurements collected during runs of a reference vehicle on the Bologna-San Donato test circuit. The developed model is validated against experimental data collected from an instrumented brake block mounted on the reference vehicle. Results show that, in spite of the simplifying assumptions, the model ensures good agreement in terms of the maximum predicted temperature.

Keywords: railway braking, tread braking, composite shoe, finite element analysis, on-track tests, experimental validation.

1 Introduction

Since the first publication of the TSI Noise regulation [1], composite materials have been replacing traditional phosphorus cast iron (P10) shoes in railway tread braking systems. While composite shoes do reduce the wheel roughness and hence the noise emission, they raise some concerns on the thermal behaviour of wheels. In fact, with respect to cast iron, composite materials typically exhibit lower thermal conductivity, which eventually leads to a higher amount of the total friction heat flux to flow towards the wheel [2]. This causes thermal stresses that can trigger thermal damage phenomena with crack nucleation/propagation [3], microstructural changes [4], as well as thermal strains that can be responsible of wheel warping with increased derailment risk [5].

Measuring the wheel temperature in operation is more difficult than measuring temperature of the brake block, because of rotation. Therefore, a detailed understanding of the thermal behaviour of brake blocks can be the key to gain indirect information on the wheel thermal field. This can thrust the identification of mitigation strategies, to promptly identify nucleation of thermal damage phenomena, as well as the optimization of maintenance operations and brake block replacement intervals. From the literature, many models exist for the prediction of the temperature field inside tread braked wheels, brake blocks or both components altogether, with the finite element (FE) method being the most common one [6,7]. The wheel temperature field is usually calculated with 2D plane [8,9], 2D axisymmetric [10,11] or 3D models [12,13]. Of course, 3D models ensure the highest computational accuracy, but they require the longest computational times. 2D plane models do not accurately represent the real thermal inertia of the wheel, while 2D axisymmetric models miss local temperature peaks and subsequent heating-cooling phases due to discontinuous contact with the blocks. The recent work by Magelli and Zampieri [14] suggests the use of harmonic axisymmetric elements to specify non-axisymmetric thermal loads over an axisymmetric geometry, thanks to Fourier series. Concerning brake blocks, different models with increasing levels of complexity and computational burden can be built. 3D models [15,16] ensure the best modelling capabilities, 2D plane models like the one shown in [17] represent a good compromise solution, despite missing heat fluxes along the axial direction, and finally 1D models are suited for integration within dynamic simulation frameworks, such as longitudinal train dynamics (LTD) [18] and multibody (MB) [19] codes.

Although several literature models exist that address thermal field calculation, and determination of wheel-block-rail heat flux partitioning, experimental validation under real operating conditions is essential to obtain reliable numerical frameworks. This works shoes a combined experimental-numerical activity. Dedicated experimental tests are performed with a reference vehicle running on the Bologna-San Donato test circuit, using a brake block with embedded thermal sensors. The results obtained from the experimental tests are compared against numerical predictions of a FE 2D plane element built as an ANSYS APDL script. The 2D plane modelling approach is selected as it ensures a good trade-off between numerical accuracy and computational efficiency.

2 Methods

2.1 Test Campaign

The experimental on-track test campaign is performed at the Bologna-San Donato railway test circuit. The main objective of the campaign is to investigate the evolution of the thermal field in a commercial K-type (high friction) composite brake shoe. The reference vehicle used in the tests is a rail grinder, with weight-on-rails of 58 ton and 1Bgu brake block configuration.

To record the internal thermal gradients along the radial and circumferential direction, two shoes mounted to the same brake block holder are instrumented with a total of eight discrete sensors, see Figure 1. These sensors are embedded at pre-defined radial depths and circumferential positions across both the upper (UP) and lower (BOT) shoes of the block unit. The sensor array comprises four Type-J thermocouples (TCJ) and four Pt1000 resistance temperature detectors (RTDs). Each individual sensor is embedded in the shoe and glued, and it is identified by a proper coloured tape wrapped around the wires. In view of their faster response time, TCJs are located as close as possible to the inner surface (around 7 mm away from the contact interface), at different circumferential positions on the upper and bottom shoes, while Pt1000 RTDs are placed at a nominal distance of 14 mm from the TCJs, to obtain the temperature gradient along the radial direction. The instrumented brake block is installed on the inner axle of the bogie below Cabin A of the reference vehicle, specifically occupying the left-hand position when the running direction is such that Cabin A is the head cabin, see Figure 2.

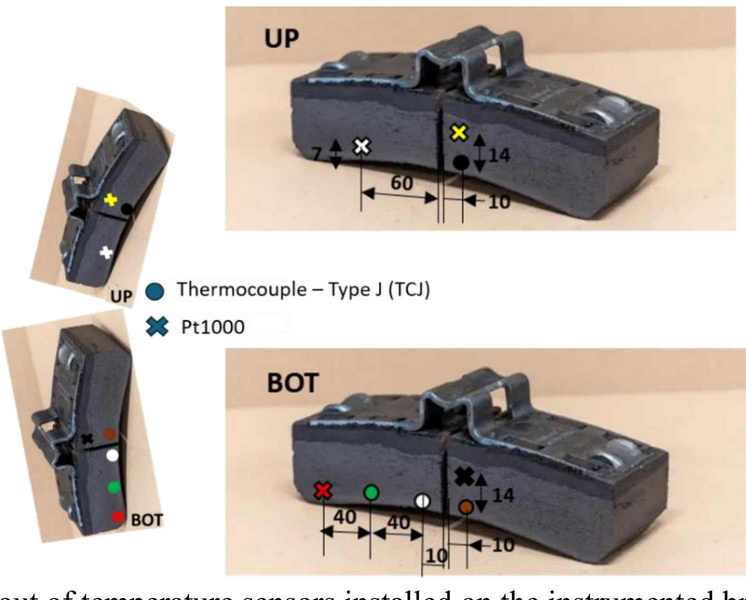

Figure 1: Layout of temperature sensors installed on the instrumented brake block.

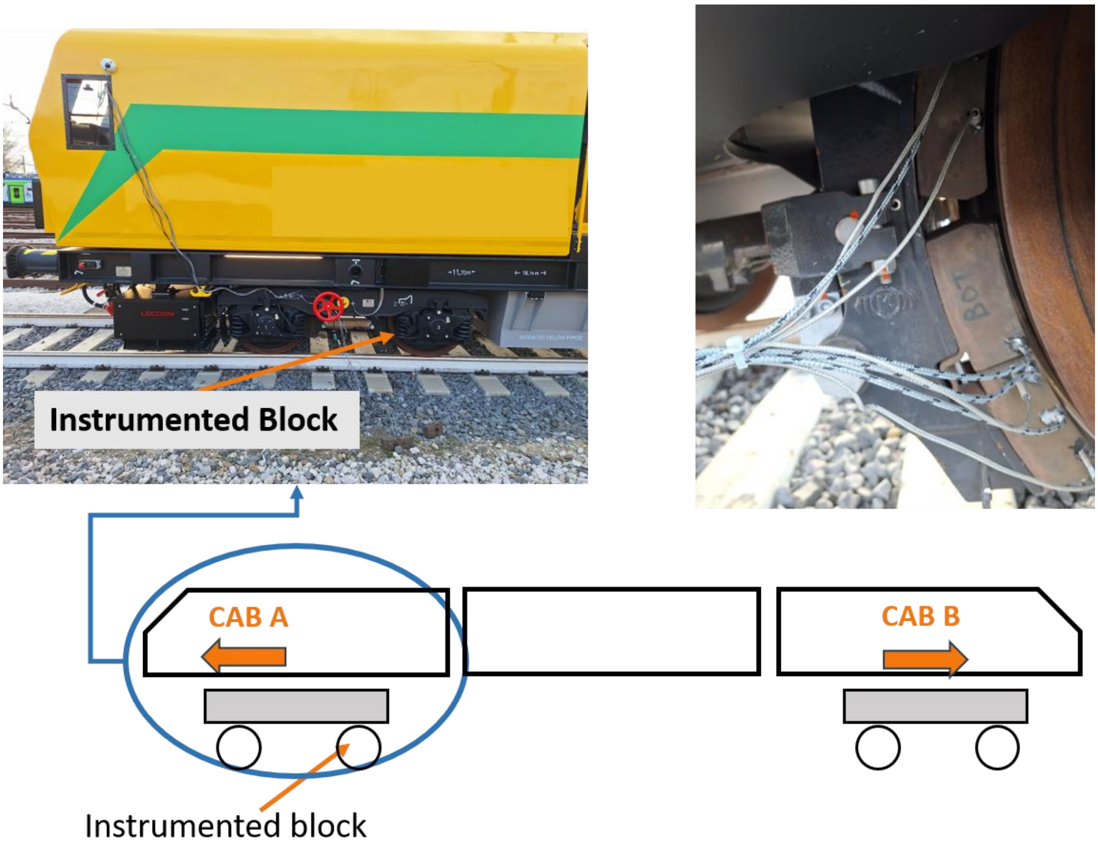

Figure 2: Installation of the instrumented brake block on the reference vehicle.

The track campaign comprises 15 independent operational runs, see Table 1. These runs explore two distinct initial speed thresholds, namely 60 and 80 km/h, which are selected based on the safety limits of the Bologna-San Donato test circuit. The tests explore both the P and G braking modes, as well as three braking modalities, i.e., automatic continuous service braking, emergency rapid braking, and direct independent braking. For each run, the following data is recorded from the on-board telemetry system:

- Initial braking speed (V_0);
- Final value of brake cylinder pressure after build-up time (p_{cyl});
- Stopping distance (s_{stop}).

Test Num.	Braking mode	Leading Cab.	Initial braking speed (km/h)	Final brake cyl. Pressure (bar)	Stopping distance (m)
1	P-Automatic	CAB A	61.1	3.44	161.7
2	P-Automatic	CAB A	80.3	3.43	306
3	P-Rapid	CAB A	61.1	3.46	149.8
4	P-Rapid	CAB A	81.4	3.46	279.1
5	P-Automatic	CAB A	61.6	3.42	166.6

6	G-Automatic	CAB A	61.4	3.38	241.4
7	G-Rapid	CAB A	62	3.42	248.5
8	G-Rapid	CAB A	80.8	3.42	423
9	G-Automatic	CAB A	80.4	3.39	429.3
10	P-Direct	CAB A	81	3.55	246.1
11	P-Direct	CAB A	60.7	3.56	118.7
12	P-Direct	CAB B	60	3.51	120.5
13	P-Direct	CAB B	80.4	3.53	217.5
14	P-Automatic	CAB B	79.7	3.44	278.2
15	No braking (convection)	CAB B	/	/	/

Table 1: Test campaign summary.

2.2 Numerical Model

A transient FE thermal model for the prediction of the brake block thermal field evolution is built as an ANSYS APDL script. To ensure high computational efficiency with good prediction capabilities, the model is built considering a 2D plane geometry, see Figure 3, under the assumption that the axial heat flux along the width of the wheel tread is negligible compared to the primary radial and circumferential fluxes.

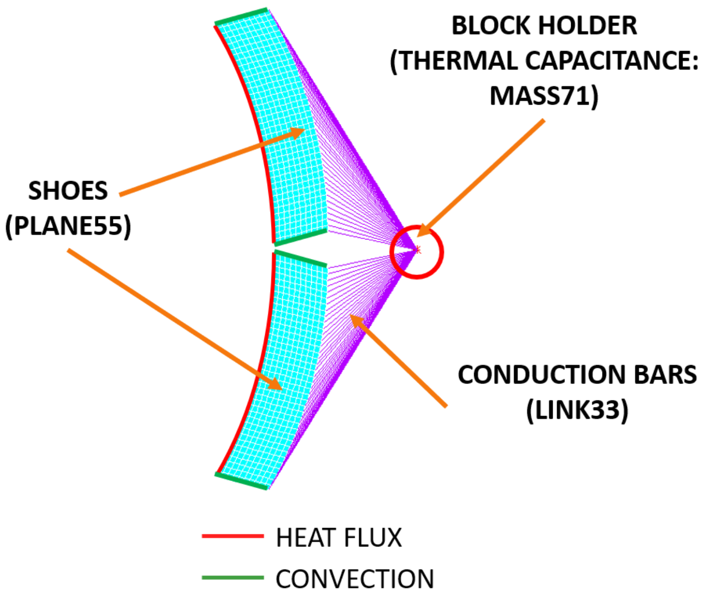

Figure 3: Schematic representation of the 2D brake block FE thermal model.

The shoes are modelled in detail meshing the geometry with 4-node planar thermal elements with linear shape functions (PLANE55). The massive cast-iron brake block holder is modelled as a lumped thermal mass node (MASS71) located at the main suspension pin attachment coordinate, connected to the outer surface of the brake shoes via uniaxial conduction bar elements (LINK33). The isotropic thermal properties assigned to the materials within the FE environment are outlined in Table 2.

Component / Material	Thermal Conductivity, W/(m·K)	Specific Heat, J/(kg·K)	Density, kg/m³
K-type shoe (composite)	0.9	1000	2000
Block holder (P10 cast iron)	48	520	7100

Table 2: Thermal properties of the materials considered in the FE model.

The total thermal capacity of the lumped holder node (C_{pc}) is computed based on its total geometric volume $V_{pc} = 1.5 \cdot 10^{-3}$ m^3, determined from mechanical drawings and yielding a value of 5538 J/K. The heat exchange area defined for the conduction links is estimated from the mechanical drawings of the block as a rectangle of length 537 mm and width 80 mm.

Two primary boundary conditions (BCs) are defined in the model during braking application. On the inner side of the shoe, that gets in contact with the wheel tread surface when braking is activated, a heat flux is prescribed and applied uniformly across the nodes. On the upper and lower sides of the shoe, forced convection cooling is implemented, considering the convection coefficient α to be governed by an empirical formulation dependent on vehicle speed, linked via the dimensionless Reynolds (Re) and Prandtl (Pr) numbers:

$$\alpha = \frac{0.037\lambda_{air}}{2R_w} Re^{0.8} Pr^{0.33} \tag{1}$$

where R_w represents the wheel radius and the air properties used are summarized in Table 3. Under standard running speeds near 70 km/h, this function yields a value of approximately 70 W/(m²·K). To account for physical uncertainties, this constant convection value is applied throughout the stop braking simulations. For the braking release phase, the heat flux BC on the inner side is removed and replaced with convection cooling.

Property (Air)	Value
Thermal Conductivity	0.026 W/(m·K)
Specific Heat	1005 J/(kg·K)
Density	1.225 kg/m^3
Dynamic Viscosity	$1.81 \cdot 10^{-5}$ Pa·s

Table 3: Physical properties of air at ambient temperature.

2.3 Determination of model inputs

For each test, the heat flux entering the brake shoe is estimated using the data collected on board the test vehicle. Since the telemetry data does not allow to acquire the time history of the brake cylinder pressure and speed, a constant average deceleration a_{med} is assumed, which is calculated as:

$$a_{med} = \frac{{V_0}^2}{2s_{stop}} \tag{2}$$

Consequently, the instantaneous vehicle speed over time t is estimated as:

$$V(t) = V_0 - a_{med}\, t \tag{3}$$

Given the total mass of the reference vehicle M_{veh}, equal to 58 ton, and assuming an identical weight distribution across all 8 wheels of the vehicle, the braking force F_{br} acting on each wheel can be estimated as:

$$F_{br} = \frac{M_{veh}}{8} \cdot a_{med} \tag{4}$$

The instantaneous dissipated power per each wheel-block contact P_{Diss} is hence evaluated as:

$$P_{Diss}(t) = F_{br} V(t) \tag{5}$$

The friction heat flux generated at the friction interface and flowing into the shoes Φ_s, which is defined as the BC applied on the inner nodes of the FE model, is then calculated as:

$$\Phi_s(t) = (1-r)\frac{P_{Diss}(t)}{2LH} \tag{6}$$

Where L is the length of a single shoe (250 mm), H is the tread width (80 mm) and r is the heat partitioning factor. The latter is calculated with a literature expression [20] as a function of the main thermal properties of wheel and shoe, and it is estimated equal to 98.19%.

3 Results

As the test are run subsequently, to comply with the time slots of the test circuit, the brake block has no time to get back to thermal equilibrium conditions, due to the low value of thermal conductivity of the composite compound. Therefore, to compare different sensor locations and different test runs, a thermal excursion is defined for each sensor and each test as:

$$\Delta T = T_{max} - T_{min} \tag{7}$$

As shown in Figure 4, in all 15 test scenarios, the maximum thermal excursion is recorded by the green TC located in the middle section of the bottom shoe, see Figure 1. This suggests that this location tends to be the critical one concerning the thermal behaviour of the shoe. On the other hand, sensors located further away from the contact surface, e.g., the yellow and black Pt1000 sensors, tend to register negligible temperature rises, due to the very low value of thermal conductivity of the composite compound. From Figure 4, it is possible to notice that, as expected, higher temperatures are reached when the faster initial speed is considered (80 km/h). Furthermore, the direct braking modality proves to be the most thermally severe, because it minimizes pneumatic delays, causing a near-instantaneous application of braking force that reduces stopping distances but amplifies the values of heat flux.

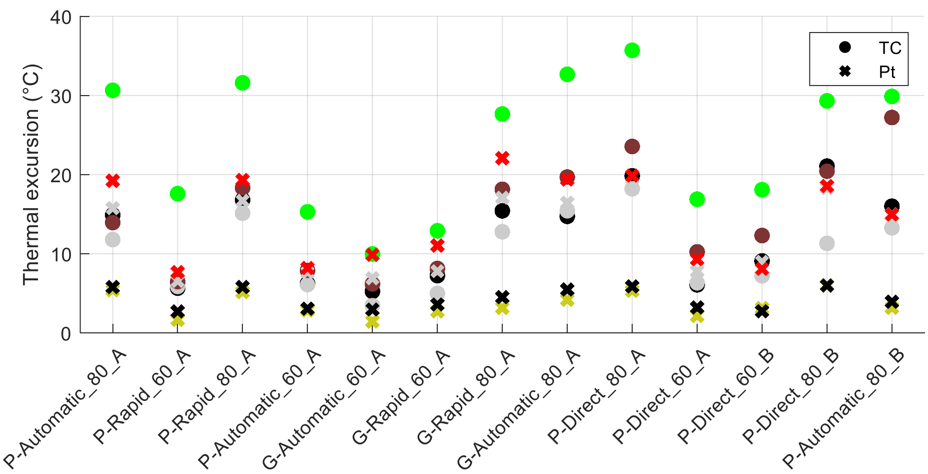

Figure 4: Temperature excursion for different braking conditions and initial speeds. Please note that each test is defined as a string like "X-Op_V_D", where "X" is the braking mode (P or G), "Op" is the braking modality, "V" is the nominal initial speed and "D" refers to the leading cabin (A or B). Different marker colours refer to the different tapes on the sensor cables, see Figure 1.

The outputs of the FE thermal models are compared with the experimental data considering the temperature calculated at the location corresponding to the green TCJ, where temperature is the highest across all tests. Figure 5 compares the temperature evolution at this location with the one obtained from the numerical simulations. A generally good agreement is identified for different braking regimes and modalities. This proves that the simplified 2D plane model can be adopted to get a good evaluation of the peak temperature that is expected in the tested braking operations.

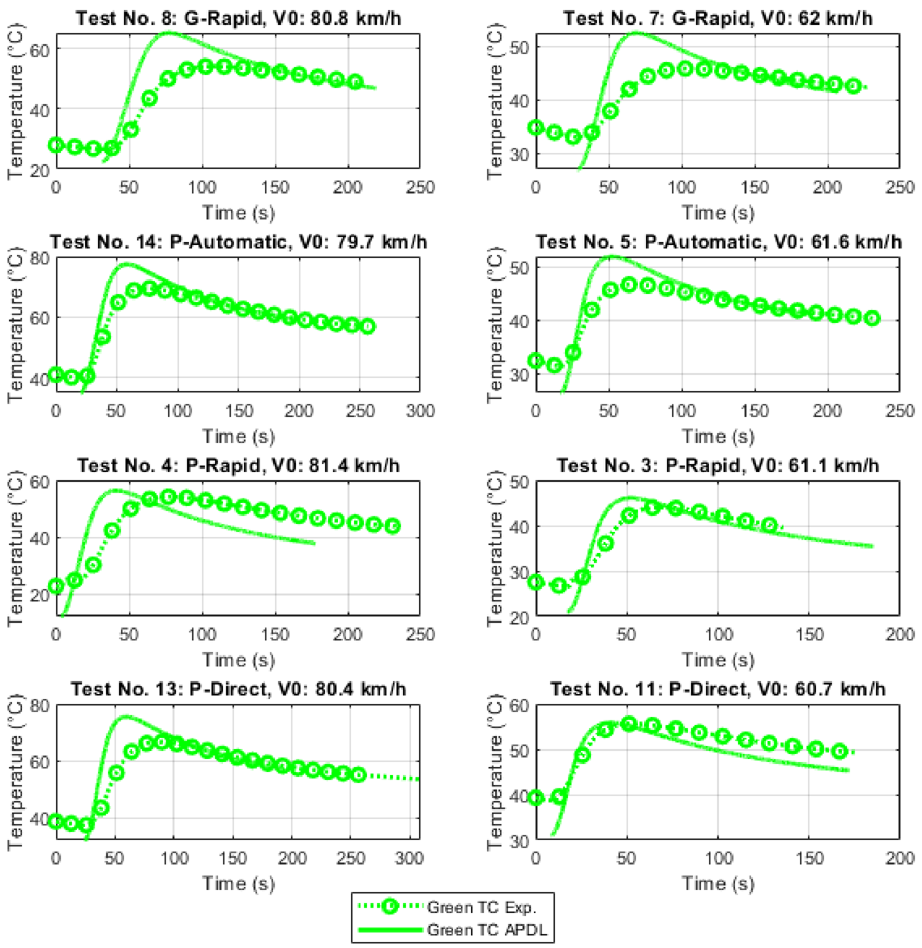

Figure 5: Comparison between numerical predictions and experimental temperature measurements at the location where the temperature is higher (Green TC).

Nonetheless, some discrepancies between experimental data and numerical predictions exists, especially for operations under the G brake mode. These differences can be related to the following reasons.

- The real brake shoe has an initial not-uniform temperature distribution due to previous braking operations, whereas, for the sake of simplicity, the FE model assumes a perfectly uniform initial temperature state equal to the average of the sensor readings. This introduces unmodeled internal conductive heat fluxes during the early stages of the experimental test.
- Small geometric misalignments exist and hence the exact position of the physical sensor was subject to drilling tolerances during block

instrumentation, meaning its location cannot perfectly match the discrete node coordinate sampled from the FE mesh.

- The numerical model operates under a simplified vehicle dynamic model assuming a constant average deceleration and a constant friction coefficient (0.3). This has a greater effect when simulating G brake mode operations, where the transient stage is not negligible due to the long build up times.

4 Conclusions

This research successfully develops and validates a 2D FE thermal model of a K-type composite railway brake shoe using experimental data from an on-track test campaign. The following conclusions can be drawn.

- The 2D plane model ensures a good compromise between numerical accuracy and computational efficiency, making it highly valuable for optimization loops and industrial design.
- The experimental tests confirm that the maximum thermal loading occurs at the mid-section of the shoe (Green TC position), while the low thermal conductivity of the composite compound reduces heating of the external layers.
- The direct braking operation represents the most critical scenario for thermal hotspot generation due to the absence of pneumatic lag and the resulting high heat generation intensity.
- The satisfactory agreement between numerical results and experimental data confirms that the model provides realistic temperature estimations at the locations where the highest temperature is recorded, despite the simplifying assumptions. This makes the model a robust tool for future safety designs of rolling stock.

Larger deviations between experimental data and numerical outputs are observed for G brake mode operations. This suggest that the model should be refined in future works to better account for transient phases of the brake application.

Acknowledgements

The authors would like to thank SRT for providing the vehicle and for enabling the railway research group at the Politecnico di Torino to take part in the tests.

References

[1] Commission Regulation (EU) of 23 December 2005 Concerning the Technical Specification for Interoperability Relating to the Subsystem 'Rolling Stock Noise' of the Trans-European Conventional Rail System. 2006

[2] G. Megna, A. Bracciali, "Tread-Braked Wheels: Review and Recent Findings", Machines, 13(7), 2025.

[3] K. Handa, Y. Kimura, Y. Mishima, "Surface cracks initiation on carbon steel railway wheels under concurrent load of continuous rolling contact and cyclic frictional heat", Wear, 268(1), 50-58, 2010.
[4] M. Faccoli, A. Ghidini, A. Mazzù, "Changes in the Microstructure and Mechanical Properties of Railway Wheel Steels as a Result of the Thermal Load Caused by Shoe Braking", Metallurgical and Materials Transactions A, 50(4), 1701-1714, 2019.
[5] M.R.K. Vakkalagadda, K.P. Vineesh., "Causes and failure forms of railway wheels", Materials Today: Proceedings, 98, 97-101, 2024.
[6] P. Wasilewski, "Frictional Heating in Railway Brakes: A Review of Numerical Models", Archives of Computational Methods in Engineering, 27(1), 45-58, 2020.
[7] L. Tran, J. Cookson, W.K Chiu, R. Saporito, "A review of thermal railway wheel modelling – Applicability and limitations", Proceedings of the Institution of Mechanical Engineers, Part F: Journal of Rail and Rapid Transit, 240(5), 539-554, 2026.
[8] A. Suresh Babu, N. Siva Prasad, "Coupled field finite element analysis of railway block brakes", Proceedings of the Institution of Mechanical Engineers, Part F: Journal of Rail and Rapid Transit, 223(4), 345-352, 2009.
[9] N. Bosso, L. Cantone, G. Falcitelli, et al., "Simulation of the thermo-mechanical behaviour of tread braked railway wheels by means of a 2D finite element model", Tribology International, 178, 2023.
[10] T. Vernersson, "Temperatures at railway tread braking. Part 1: Modelling", Proceedings of the Institution of Mechanical Engineers, Part F: Journal of Rail and Rapid Transit, 221(2), 167-182, 2007.
[11] R. Siniscalchi, L. Cantone, "Two fast models to compute the thermal field in wagons with brake blocks via finite differences", Proceedings of the Institution of Mechanical Engineers, Part F: Journal of Rail and Rapid Transit, 239(3), 211-221, 2025.
[12] M. Milošević, D. Stamenković, M. Tomić, et al., "Modeling thermal effects in braking systems of railway vehicles", Thermal Science, 16(2), 515-526, 2012.
[13] S. Pradhan, A.K. Samantaray, "A Recursive Wheel Wear and Vehicle Dynamic Performance Evolution Computational Model for Rail Vehicles with Tread Brakes", Vehicles, 1(1), 88-115, 2019.
[14] M. Magelli, N. Zampieri, "A new finite element axisymmetric model with non-axisymmetric thermal loads for thermal analyses of tread braked wheels", Tribology International, 209, 2025.
[15] N. Békési, K. Váradi, "Contact thermal analysis and wear simulation of a brake block", Advances in Tribology, 2013.
[16] A. Somà, M. Aimar, N. Zampieri, "Simulation of the Thermal Behavior of Cast Iron Brake Block during Braking Maneuvers", Applied Sciences, 11(11), 2021.
[17] M. Magelli, R. Pagano, N. Zampieri, "Adapting a scaled twin-disc device for tread braking investigations based on an ad-hoc thermal similitude model", Wear, 574-575, 2025.

[18] Q. Wu, M Magelli, N. Zampieri, E. Bernal, "Adding a brake shoe temperature model into freight train longitudinal braking dynamics simulations", Proceedings of the Institution of Mechanical Engineers, Part F: Journal of Rail and Rapid Transit*,* 237(5), 631-641, 2023.
[19] M.R.K. Vakkalagadda, K.P. Vineesh, V. Racherla, "Estimation of railway wheel running temperatures using a hybrid approach", Wear, 328-329, 537-551, 2015.